DOUBLE-HYPERBOLIC FORCE–VELOCITY RELATION IN FROG MUSCLE FIBRES

By K. A. P. EDMAN

From the Department of Pharmacology, University of Lund, Sölvegatan 10, S-223 62 Lund, Sweden

SUMMARY

1. The relationship between force and velocity of shortening was studied at $2.10\ \mu m$ sarcomere length during fused tetani (1–3 °C) in single fibres isolated from the anterior tibialis muscle of *Rana temporaria*. The speed of shortening was recorded from the whole fibre and, in some experiments, simultaneously from a short (*ca.* 0·6 mm) segment, while the preparation was released to shorten isotonically at selected force levels ('load-clamp' recording). The segment was defined by opaque markers of hair that were placed on the fibre surface. The distance between the markers was recorded by means of a photo-electric detector system.

2. The force–velocity relation had two distinct regions, each one exhibiting an upwards concave shape, that were located within the ranges 0–78 and 78–100 % of the measured isometric force (P_0), respectively. The two portions of the force–velocity relation could be fitted well by hyperbolic functions or by single-exponential functions. The curvature was more pronounced in the high-force region than at low–intermediate loads. The transition between the two portions of the force–velocity relation (the 'break point' of the force–velocity curve) occurred at $78.4 \pm 0.4\%$ of P_0 (mean $\pm$ S.E. of mean, $n = 12$) corresponding to $10.9 \pm 0.4\%$ of maximum velocity of shortening (V_{max}). The general shape of the force–velocity curve, and the appearance of a break point near 78 % of P_0, was the same when measurements were made from the whole fibre and from a short segment along the same fibre.

3. The 'negative' branch of the force–velocity relation was delineated for loads ranging from P_0 to 1.6–$1.8\ P_0$ in five experiments. The negative branch formed a smooth continuation of the force–velocity relation recorded between $0.78\ P_0$ and P_0. The force–velocity relation was nearly flat between $0.90\ P_0$ and $1.20\ P_0$, the difference in speed of shortening or elongation being $1.8 \pm 0.3\%$ (mean $\pm$ S.E. of mean, $n = 5$) of V_{max} over this range.

4. An increase in sarcomere length from 1·85 to 2·60 μm did not affect V_{max} but caused a steady decrease in curvature of the force–velocity relation, both at low–intermediate loads and in the high-force range. Similar changes in shape of the force–velocity relation were produced by osmotic compression of the fibre in a Ringer solution made hypertonic by addition of 98 mM-sucrose. The position of the break point of the force–velocity relation was not significantly affected by altered tonicity or altered sarcomere length, nor by a change in temperature from 1·8 to 11·0 °C.

5. A modified version of Hill's (1938) hyperbolic equation was used to fit the experimental data and to express the interrelation between the two portions of the force–velocity curve on either side of the break point. The interrelation between the two portions was quite similar from fibre to fibre and remained constant in any given fibre under conditions where the overall shape of the force–velocity curve was markedly changed.

6. The results suggest that the kinetics of cross-bridge function is changed as the load exceeds approximately 78 % of the measured isometric force.

INTRODUCTION

Unlike a simple elastic body, muscle is able to adjust its force to precisely match the load that is experienced during shortening. This remarkable property of muscle is based on the fact that active force continuously adjusts to the speed at which the contractile system moves. Thus, when the load is small, the force produced by the muscle is made correspondingly small by increasing the speed of shortening appropriately. Conversely, when the load is high, the active force is raised to an equivalent level by decreasing the shortening speed sufficiently. The fact that there exists a given relation between load and velocity of shortening in muscle was first demonstrated by Fenn & Marsh (1935). Hill (1938) further characterized the force–velocity relation in frog skeletal muscle and pointed out the importance of this parameter for understanding the basic mechanisms of muscle contraction. Much new interest has been focused on the force–velocity relation in recent years after it had become clear (Huxley, 1957) that this relationship is consistent with a sliding-filament mechanism that is based on independent force generators (Huxley & Niedergerke, 1954; Huxley & Hanson, 1954).

Previous studies on isolated whole muscles of the frog have shown that the force–velocity relation can be adequately described as part of a rectangular hyperbola (Hill, 1938; Jewell &Wilkie, 1958; Ritchie & Wilkie, 1958). Experiments on isolated single muscle fibres confirmed the hyperbolic nature of the force–velocity relation at low and intermediate loads but demonstrated that the force–velocity behaviour undergoes a clear change as the load is raised above 80 % of maximum isometric force (Edman, Mulieri & Scubon-Mulieri, 1976). This observation opened the possibility that the kinetics of the cross-bridges might change as the load on the muscle exceeds a critical level.

The present study was undertaken to explore the force–velocity relation in the high-force range in further detail using techniques that enabled measurements both from the fibre as a whole and from a short segment along the intact fibre. Results will be presented to show that the kinetics of steady shortening is changed in a specific way as the load is increased beyond 78 % of the isometric force. Experiments were designed to determine if this change in force–velocity behaviour in the high-force range is dependent on filament overlap and myofilament lattice width. Some of the results have been previously reported in a preliminary form (Edman, 1986, 1988).

METHODS

Preparation, mounting and stimulation

Experiments were performed on muscles from *Rana temporaria* that had been stored at about +4 °C for at least 7 days before use. Single fibres were dissected from the anterior tibialis muscle using fine-tipped scissors, and care was taken to avoid any appreciable stretching of the fibre during the dissection procedure. The fibres were mounted horizontally in a thermostatically controlled Perspex chamber between a force transducer (AE 801, Aksjeselskapet Mikroelektronikk, Horten, Norway) and an electromagnetic puller as described earlier (Edman & Reggiani, 1984). With the technique used (tendons held by aluminium clips) it was possible to minimize any lateral and vertical motion, or twisting, of the fibre during the onset of contraction. The sideways movement of the fibre during an isometric contraction was < 15 μm as measured near the tendon insertions.

The bathing solution had the following composition (mM): NaCl, 115·5; KCl, 2·0; CaCl$_2$, 1·8; Na$_2$HPO$_4$–NaH$_2$PO$_4$, 2·0; pH, 7·0. The solution was pre-cooled and perfused through the muscle chamber (volume *ca.* 2·5 ml) at a speed of approximately 5 ml/min. The temperature of the bathing solution was held constant to ±0·1 °C throughout an experiment but ranged, unless otherwise stated, from 1·0 to 3·3 °C in the whole series of experiments.

In one set of experiments the tonicity of the extracellular medium was increased by adding 98 mM-sucrose to the Ringer fluid. The osmotic strength of the sucrose-containing medium was calculated to be 1·44 × that of the normal Ringer solution (*R*) (Edman & Hwang, 1977).

Cross-sectional area and fibre length were measured as described by Edman & Reggiani (1984). Sarcomere length was determined by laser diffraction technique (Cleworth & Edman, 1972).

The fibre was stimulated by passing rectangular pulses of current (0·2 ms duration) between two platinum plate electrodes that were placed symmetrically on either side of the preparation approximately 2 mm from it. The stimulus strength was approximately 20 % above the threshold. A train of pulses of appropriate frequency (16–22 Hz) was used to produce a fused tetanus of 0·5 or 1·0 s duration. The pulse frequency used was just sufficient to achieve complete mechanical fusion in the individual fibre at the sarcomere length considered. The fibre was stimulated at regular, 2 min intervals throughout the experiment.

Load-clamp recording

The electromagnetic puller used in this study has been described (Edman & Reggiani, 1984). Load clamping for isotonic shortening was performed by rapidly changing the mode of operation of the puller from fibre-length control to force control. The switch-over to force control occurred during the plateau of the tetanus (*ca.* 350 ms after the onset of stimulation) and the force-control mode was thereafter maintained for the remainder of the tetanus period. With the experimental device used it was possible to achieve stable clamp tension over a wide force range, even very close to zero force level.

Segment length recording

In some experiments changes in length of a discrete segment of the intact muscle fibre were recorded during load clamping using the surface marker technique previously described (Edman & Reggiani, 1984). The segment was delineated by two opaque markers that were cut from black dog's hair and placed *ca.* 0·6 mm apart on the upper surface of the fibre. The accuracy of the segment length measurement was better than 0·2 % of the segment's length, and the time resolution was 250 μs. In later experiments of the series the time resolution of the segment length measurement was 40 μs. This increase in time resolution was achieved by using a Fairchild CCD133 photodiode array for the read-out of the marker positions along the fibre.

Analysis of data

Outputs from the force and displacement transducers and the photodiode array (Reticon CCPD 1024 or Fairchild CCD133) were displayed on Tektronix 5113 storage oscilloscopes and photographed on 35 mm film. The film records were measured on a Nikon profile projector using the stage micrometer readings as previously described (Edman, 1979). The slopes of the shortening records obtained from the displacement transducer of the puller (overall fibre length) and the photodiode array (segment length change) were measured to the nearest minute of arc on the Nikon

vernier scale and were converted to muscle lengths per second (L/s). Such measurements were performed within the straight portion of the shortening records no earlier than 20 ms after the release. In cases where oscillations were still visible at this time (see the first section of Results) the average slope of the trace was determined by interpolation. In later experiments signals were recorded and measured using a Nicolet 4094 B digital oscilloscope provided with a disc recorder.

The force–velocity data were fitted by Hill's (1938) hyperbolic equation using a method of three-dimensional regression analysis (K. A. P. Edman & B. Wohlfart, unpublished). The fitting procedure minimized the squares of the deviations about power (force × velocity). The analytical results derived by this method agreed closely with those obtained by the reiterative computer routine previously used (Edman et al. 1976). The Hill (1938) equation is given by

$$(P+a)(V+b) = (P_0+a)b, \tag{1}$$

in which P_0 is the measured isometric force, P the load on the muscle fibre, V the velocity of shortening and a and b are constants with dimensions of force and velocity, respectively. The velocity of shortening at zero load, V_{max}, was estimated from a hyperbola that was fitted to force–velocity data truncated at 78 % of P_0.

Student's t test was used for determinations of statistical significance. All statistics are given as mean ± S.E. of mean.

<center>RESULTS</center>

Shortening of whole fibre and fibre segment during load clamp

Sample load-clamp recordings from a whole muscle fibre and from a short segment of the same (intact) fibre are illustrated in Fig. 1A–C. As can be seen, constant force could be attained at any selected level within 10–30 ms after switching to force-control mode of the electromagnetic puller. The length signals of the whole fibre and of the segment had similar features. They both contained an initial rapid phase which coincided with the steep change in tension at the onset of force clamp. This initial length change is attributable to recoil of elastic components, i.e. in the case of the segment length recording, recoil of elastic structures that reside inside the sarcomere units. The second shortening phase started with a damped oscillation which formed a smooth continuation of the initial phase. At an appropriate feed-back control of the electromagnetic puller the length oscillation was of a small amplitude and generally did not persist over more than one cycle. The period of the oscillation was 7–8 ms near zero load and ca. 80 ms close to isometric force. These times accord with previous measurements on intact muscle fibres (Civan & Podolsky, 1966; Sugi & Tsuchiya, 1981). The slope of the shortening record stayed constant over a fairly large interval after the initial oscillations had faded out. The velocity of shortening during this straight portion of the shortening ramp was used for the analysis of the force–velocity relation (see Methods).

In occasional fibres load clamping at the greatest loads (ca. 0·9 P_0 and higher) gave rise to damped length oscillations that did not fully disappear during the load-clamp period (Fig. 1D). A similar observation has previously been reported by Armstrong, Huxley & Julian (1966). The relatively short period of the oscillations made it nevertheless feasible to determine, with sufficient accuracy, the *average* slope of the shortening record by interpolation. The results from such fibres did not in any obvious way differ from those obtained in preparations where oscillations were virtually absent.
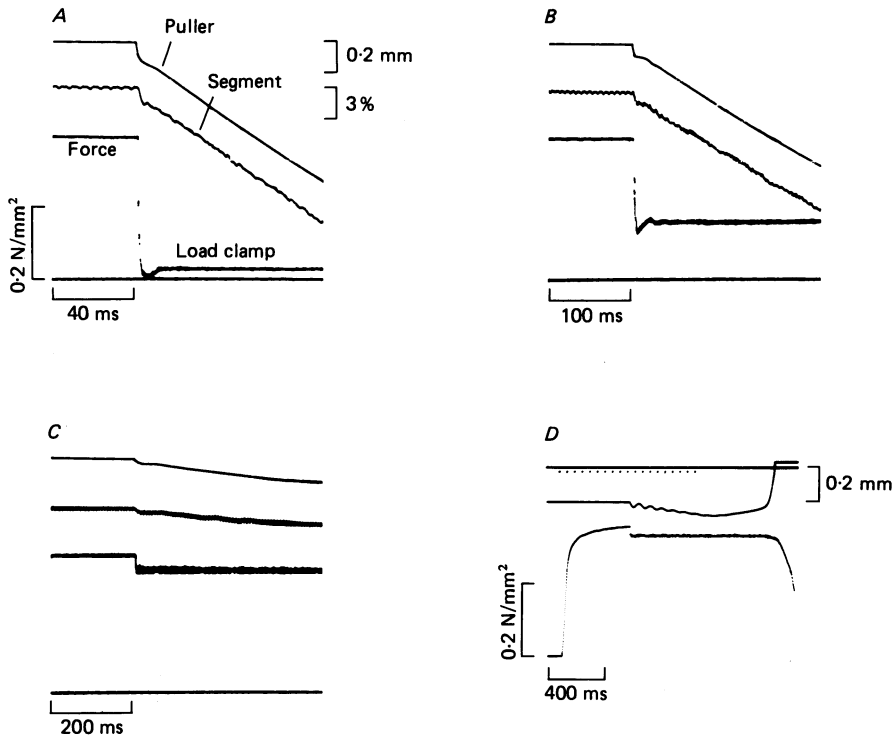
Fig. 1. *A–C*, examples of load-clamp recordings at three different force levels during tetanus of a single muscle fibre. In each set of records traces represent from top: fibre length (puller signal), segment length and force. Calibrations of the signals are the same in *A–C* but note differences in time base. Downward deflections of puller signal (millimetres) and segment length recording (per cent) indicate shortening. Resting sarcomere length: 2·10 μm. Fibre length: 6·30 mm. Temperature: 2·2 °C. *D*, load-clamp recording in fibre that produced oscillations throughout the shortening phase at high ($> 0.9\,P_0$) loads. Traces from top: stimulation signal (dots), fibre length (puller signal) and force. Resting sarcomere length: 2·10 μm. Fibre length: 7·50 mm. Temperature: 1·8 °C.

Differential shape of the force–velocity relation at low–intermediate and high loads

Figure 2 illustrates force–velocity data obtained from a whole single muscle fibre (*A*) and from a segment (*ca.* 0·6 mm in length) of the same intact fibre (*B*). The measurements were performed at 2·10 μm sarcomere length. In both cases the force–velocity relation exhibits two distinct curvatures located on either side of a break point near 78 % of the measured isometric force, P_0. The high-force curvature is more pronounced than that at low–intermediate loads resulting in a marked change in slope between the two branches of the force–velocity relation at the point of transition.

In confirmation of previous results (Edman *et al.* 1976), Hill's (1938) hyperbolic equation provides an excellent fit to velocity data truncated at $0.78\,P_0$. The hyperbola so derived intersects the force axis at a point (P_0^*) that is markedly higher than P_0. In thirteen experiments, performed at 2·10 μm sarcomere length, P_0^* was
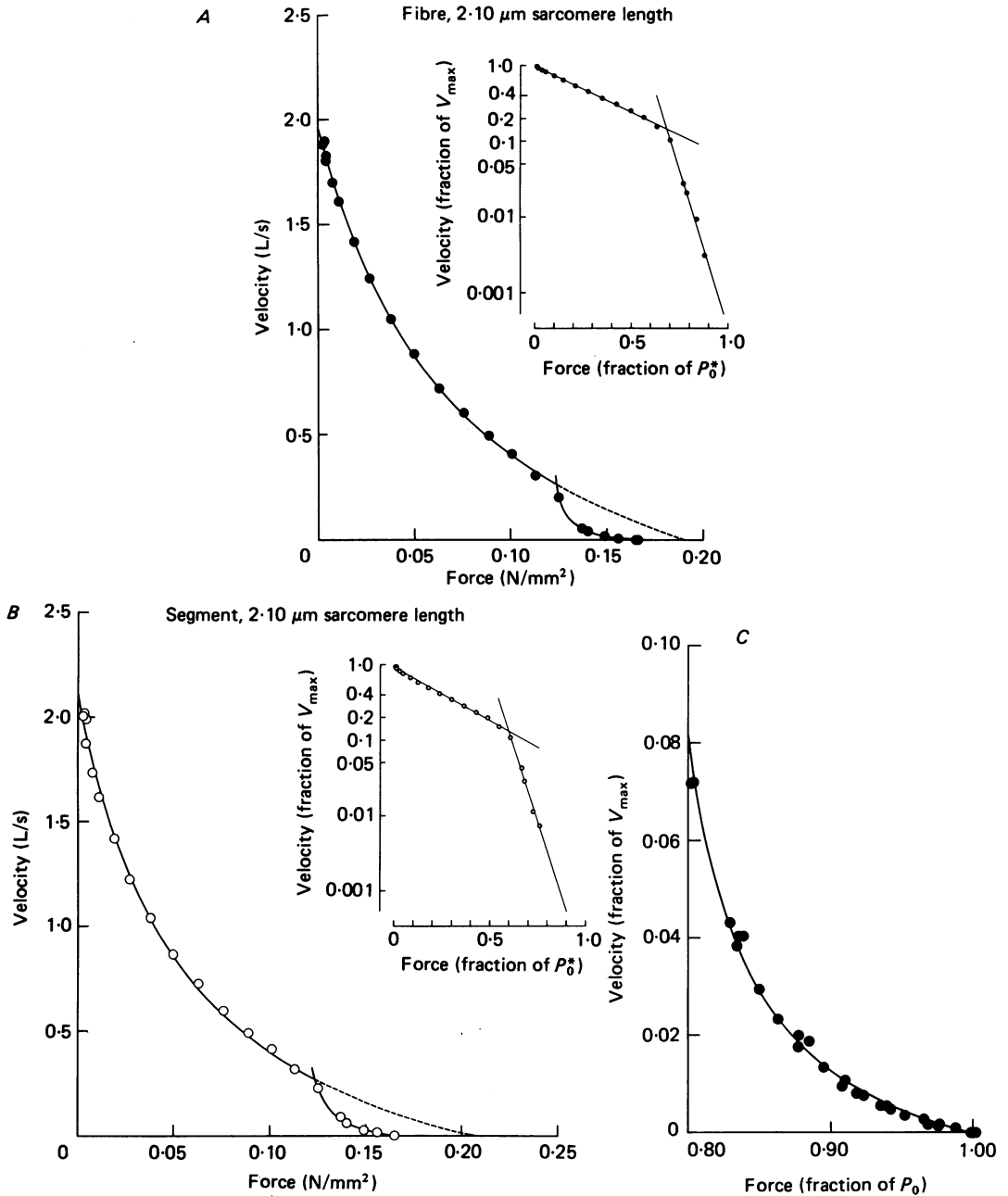
Fig. 2. *A* and *B*, force–velocity curves based on load-clamp recordings in a single muscle fibre. Velocity of shortening recorded in the fibre as a whole (*A*) and in a short (*ca.* 0·6 mm) segment of the same fibre (*B*). Note difference in curvature of force–velocity relation on either side of a break point near $0·78 P_0$. Continuous lines: Hill's hyperbolic equation fitted to data points above and below the break point. The value of a/P_0^* is 0·40 in *A* and 0·28 in *B*. Insets: semilogarithmic plots of force–velocity data given in main diagrams. Lines in the insets, linear regressions of velocity upon force on either side of the break point. Sarcomere length: 2·10 μm. Temperature: 2·2 °C. *C*, force–velocity data derived in high-force range plotted in diagram in which ordinate has been placed at $0·80 P_0$. Data refer to whole-fibre measurements. Hyperbola fitted by least-squares method; correlation coefficient 0·97. Sarcomere length: 2·10 μm. Temperature: 3·4 °C.

$17 \pm 1 \%$ higher than P_0 (Table 1). The results presented in Fig. 2 *A* and *B* furthermore demonstrate that the high-force portion of the force–velocity relation can also be fitted well by a hyperbolic function. This is further illustrated in Fig. 2 *C* in which high-force data obtained from repeated measurements in one fibre have been plotted in a separate diagram. Here the ordinate has been arbitrarily placed at $0.80\,P_0$, i.e. close to the break point of the force–velocity relation. As can be seen Hill's hyperbolic equation provides a good fit to the data points, the correlation coefficient being 0.97.

The existence of two distinct portions of the force–velocity relation is further illustrated in the insets of Fig. 2, where the force–velocity data shown in the main diagrams have been replotted in semilogarithmic graphs. As can be seen, each of the two portions of force–velocity data (located on either side of the break point near 78% of P_0) can be fitted quite well with a single-exponential function that relates shortening velocity to active force. Small systematic deviations of the experimental values do exist along the calculated lines. However, the overall difference in slope between the two portions is unmistakable in this linearized plotting.

The break point of the force–velocity relation was determined from the intersection of the two regression lines in semilogarithmic plottings like those illustrated in Fig. 2 (insets). According to such measurements performed at $2.10\,\mu$m sarcomere length in ordinary Ringer solution the break point of the force–velocity curve was located at $78.4 \pm 0.4\%$ of P_0 and $10.9 \pm 0.4\%$ of V_{max} ($n = 12$).

The curvature of the force–velocity relation at low–intermediate loads is given by the ratio a/P_0^* in Hill's (1938) hyperbolic equation fitted to data points below $0.78\,P_0$. The value of a/P_0^* increases with decreasing curvature. A similar quantitative expression for the *high-force* curvature is difficult to achieve on the basis of a hyperbolic fitting due to the fact that the co-ordinates pertaining to the rectangular hyperbola at high loads can only be defined approximately for the individual fibre. Evidence will be presented to show, however, that the two portions of the force–velocity curve are closely related to one another and that this interrelation is maintained under different experimental conditions that markedly affect the overall shape of the curve (see section 'Curve fitting of force–velocity data').

Length dependence of force–velocity relation

Figure 3 illustrates force–velocity data collected at four different lengths within the range 1.85–$2.60\,\mu$m. The measurements were restricted to this range of sarcomere lengths in order to avoid interference from resting tension that becomes appreciable at lengths greater than $2.70\,\mu$m and passive resistive forces that appear at sarcomere lengths shorter than $1.70\,\mu$m (see Edman, 1979). For load-clamp recording at $1.85\,\mu$m sarcomere length, i.e. below slack length, the tetanus was initiated at $2.10\,\mu$m, and the fibre was allowed to shorten to develop full isometric force at the new length (see further Methods).

As can be readily seen from Fig. 3, an increase in sarcomere length from 1.85 to $2.60\,\mu$m was associated with a steady decrease in curvature of the force–velocity relation, both at low–intermediate loads (i.e. below $0.78\,P_0$) and in the high-force range. By this change in shape of the force–velocity relation the difference in curvature on either side of the break point became less conspicuous as the sarcomere length was increased. The decrease in curvature of the force–velocity relation at
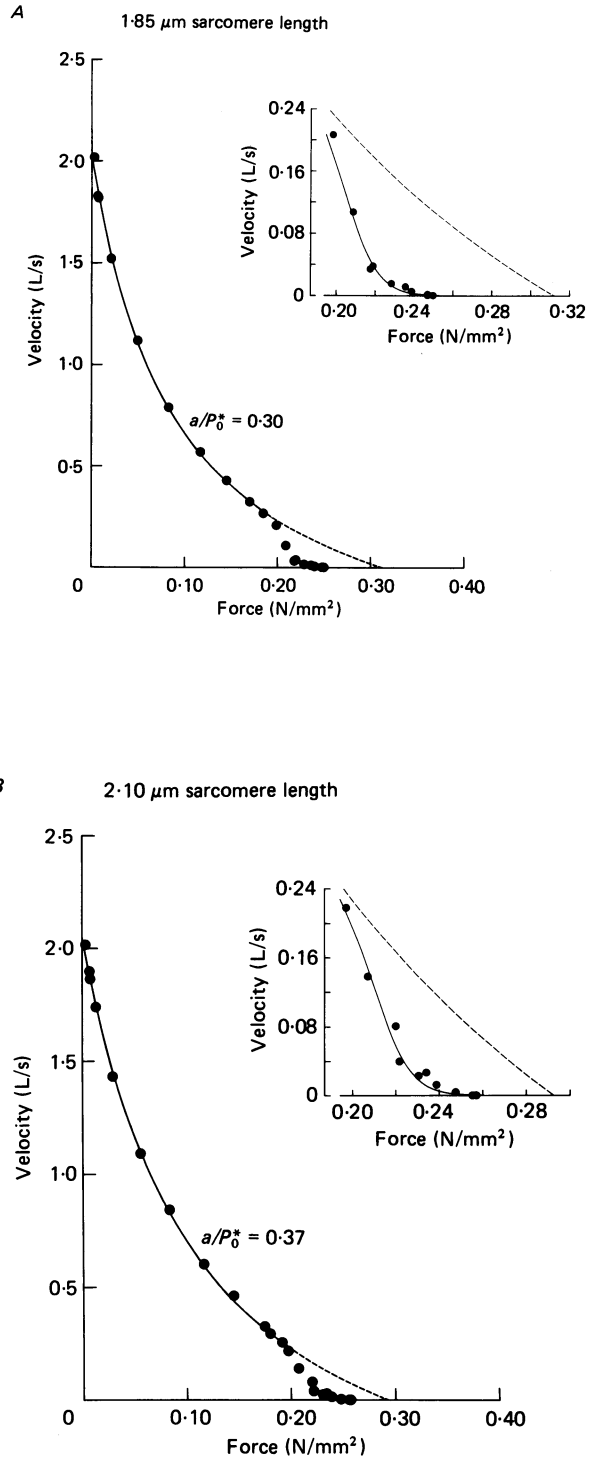
A

1·85 μm sarcomere length

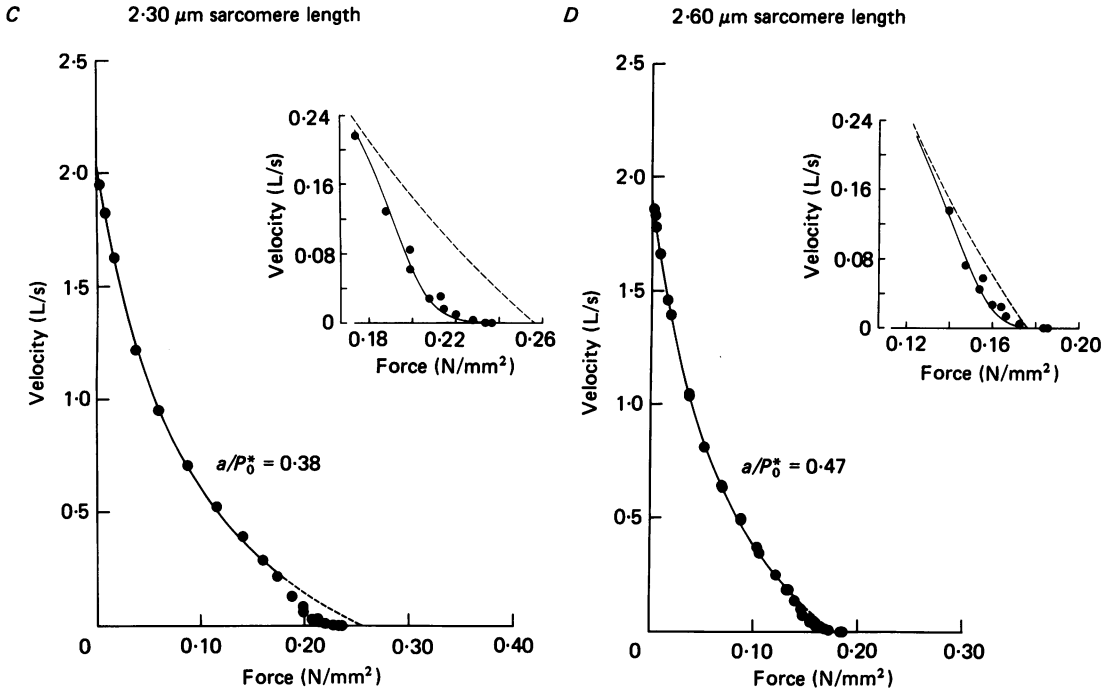
B

2·10 μm sarcomere length

Fig. 3. For legend see opposite.

Fig. 3. Force–velocity relations in a single muscle fibre at four different sarcomere lengths: 1·85 μm (*A*), 2·10 μm (*B*), 2·30 μm (*C*) and 2·60 μm (*D*). Hyperbolas fitted to data truncated at 0·78 P_0. Insets: detail of high-force portion of the force–velocity relation shown in main diagram. Dashed line, hyperbola derived from data below 0·78 P_0. Continuous line in the insets, eqn (2) (see Results) fitted to force–velocity data using the same numerical values for k_1 (125 mm^2/N) and k_2 (0·84) in *A–D*. Note steady decrease in curvature of both sections of the force–velocity relationship as sarcomere length is increased. Temperature 1·0 °C.

greater lengths furthermore had the consequence that P_0^* (the force intercept extrapolated from data at low and intermediate loads) more closely approached the *measured* value of the isometric force, P_0. At 2·60 μm sarcomere length P_0^* coincided with P_0 (Fig. 3*D* and Table 1). The value of a/P_0^* (expressing the curvature at low–intermediate loads) rose by 26±7 % ($P < 0·01$, $n = 9$, paired observations) as the sarcomere length was increased from 2·10 to 2·60 μm.

The break point of the force–velocity relation, measured at 2·60 μm sarcomere length, occurred at 76·4±1·0 % of P_0 and 10·6±0·9 % of V_{max} ($n = 9$). These values are not significantly different from those recorded at 2·10 μm sarcomere length (see section 'Differential shape of the force–velocity relation at low–intermediate and high loads').

V_{max}, the estimated value of maximum velocity of shortening (see Methods) was not markedly changed between 1·85 and 2·60 μm sarcomere length in accordance with previous observations (Edman, 1979). In seven experiments V_{max} measured at 2·60 μm sarcomere length was 1·00±0·02 (paired observations) of the value recorded at 1·85 μm.

The force–velocity relation at varied tonicity of the extracellular medium

As an intact muscle fibre maintains a virtually constant volume during a length change, the diameter of the fibre, and therefore the width of the myofilament lattice (Huxley, 1953; Elliott, Lowy & Worthington, 1963; Elliott, Lowy & Millman, 1967), has been shown to vary as an inverse square root function of the sarcomere length. Experiments were performed to test whether the length-induced changes of the force–velocity relation described in the preceding section may be reproduced by altering the fibre width *per se* while keeping the sarcomere length constant. To this end force–velocity measurements were carried out in five experiments at $2 \cdot 10 \; \mu$m sarcomere length after equilibrating the fibre in ordinary Ringer solution (tonicity $1 \cdot 00 \; R$) and in a Ringer solution made hypertonic ($1 \cdot 44 \; R$) by addition of 98 mM-sucrose. The increase in tonicity so produced would cause approximately 20 % decrease in the fibre cross-sectional area (Blinks, 1965) which corresponds closely to the change in fibre width that occurs as the sarcomere length is increased from $2 \cdot 1$ to $2 \cdot 6 \; \mu$m.

TABLE 1. Force–velocity parameters recorded in single muscle fibres in normotonic ($1 \cdot 00 \; R$) and hypertonic ($1 \cdot 44 \; R$) medium and at varied sarcomere length (SL)

Tonicity	SL (μm)	V_{max} (L/s)	a/P_0^*	P_0^*/P_0	Number of experiments
$1 \cdot 00 \; R$	$1 \cdot 85$	$1 \cdot 91 \pm 0 \cdot 06$	$0 \cdot 32 \pm 0 \cdot 02$	$1 \cdot 20 \pm 0 \cdot 01$	7
$1 \cdot 00 \; R$	$2 \cdot 10$	$2 \cdot 01 \pm 0 \cdot 05$	$0 \cdot 33 \pm 0 \cdot 02$	$1 \cdot 17 \pm 0 \cdot 01$	13
$1 \cdot 00 \; R$	$2 \cdot 60$	$1 \cdot 90 \pm 0 \cdot 04$	$0 \cdot 44 \pm 0 \cdot 03$	$0 \cdot 98 \pm 0 \cdot 02$	9
$1 \cdot 44 \; R$	$2 \cdot 10$	$1 \cdot 36 \pm 0 \cdot 07$	$0 \cdot 49 \pm 0 \cdot 05$	$1 \cdot 00 \pm 0 \cdot 03$	5

V_{max} and P_0^* denote maximum speed of shortening and maximum force, respectively, estimated from hyperbola fitted to force–velocity data within the range 0–78 % of measured isometric force (P_0). a/P_0^* is the force asymptote of this hyperbola (cf. Fig. 2). Mean $\pm$ S.E. of mean.

Results from a typical experiment are presented in Fig. 4. In accordance with previous results (Howarth, 1958; Edman & Hwang, 1977) V_{max} and P_0 both decreased by immersing the fibre in the hypertonic solution. In five experiments (paired observations) the mean reductions of V_{max} and P_0 were 33 ± 4 and $22 \pm 2 \%$, respectively. Hypertonicity furthermore altered the *shape* of the force–velocity relation in a way that was strikingly similar to that produced by increased sarcomere length as is shown in Fig. 4 and Table 1. There was a consistent decrease in curvature of the force–velocity relation, both at low–intermediate loads and in the high-force range. The value of a/P_0^* measured in the hypertonic medium was $55 \pm 7 \%$ ($P < 0 \cdot 01$, $n = 5$, paired observations) higher than that recorded in normal Ringer solution. Furthermore, the ratio P_0^*/P_0 was reduced to a value close to unity in the hypertonic solution.

The break point of the force–velocity relation was located at $77 \cdot 2 \pm 0 \cdot 6 \%$ of P_0 and $11 \cdot 0 \pm 0 \cdot 7 \%$ of V_{max}. These values are not significantly different from those measured in the ordinary Ringer solution (see section 'Differential shape of the force–velocity relation at low–intermediate and high loads').
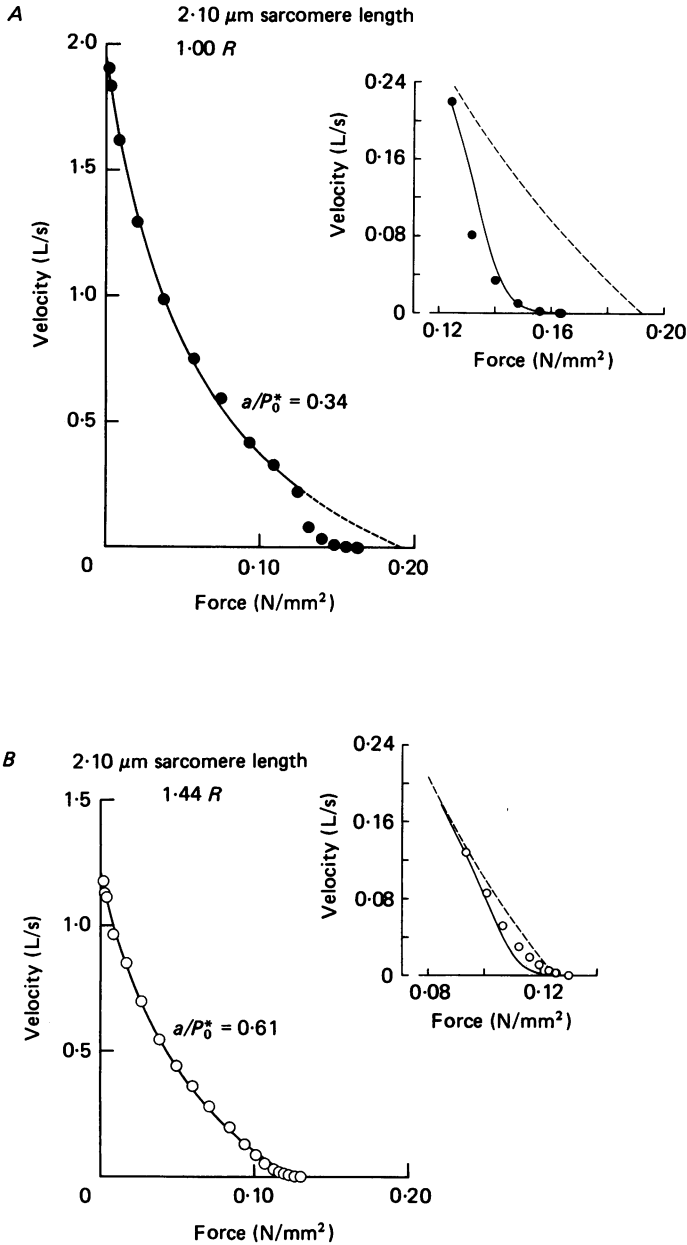
Fig. 4. Force–velocity relations in a single muscle fibre: A, in isotonic ($1·00\ R$) Ringer solution and B, in $1·44\ R$ hypertonic medium. Hyperbolas fitted to data truncated at $0·78\ P_0$. Insets: detail of high-force portion of the force–velocity relation shown in main diagram. Dashed line, hyperbola derived from data below $0·78\ P_0$. Continuous line in the insets, eqn (2) (see Results) fitted to force–velocity data using the same numerical values for k_1 ($200\ \text{mm}^2/\text{N}$) and k_2 ($0·83$) in both A and B. Note that hypertonicity causes a decrease of both V_{max} and P_0 and a decrease in curvature of both portions of the force–velocity relation. Sarcomere length: $2·10\ \mu\text{m}$. Temperature: $1·6\ °\text{C}$.
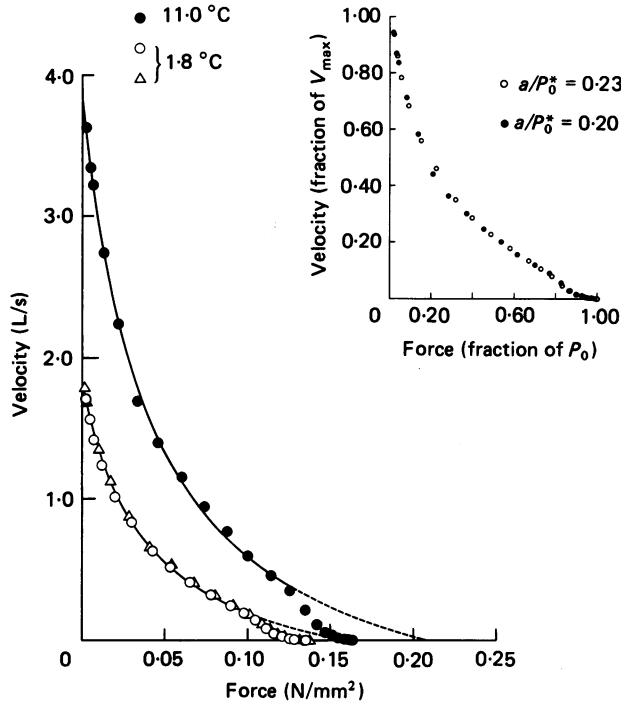
Fig. 5. Influence of temperature on force–velocity relation in a single muscle fibre. $\bigcirc$, 1·8 °C; $\bullet$, 11·0 °C; $\triangle$, return to 1·8 °C. Hyperbolas fitted to data truncated at 0·78 P_0. Inset: data in main diagram normalized with respect to V_{max} and P_0 at respective temperature. Sarcomere length: 2·10 μm.

Influence of temperature on the force–velocity relation

Previous experiments on both whole muscle and single fibres have shown that the overall shape of the force–velocity relation is not critically dependent on temperature (for references, see Woledge, Curtin & Homsher, 1985). It was of interest to find out if the two portions of the force–velocity relation described in preceding sections were influenced to the *same* degree by a temperature change. Figure 5 illustrates results from an experiment in which three complete series of force–velocity measurements were carried out at the following temperatures: (a) 1·8 °C, (b) 11·0 °C and (c) return

Fig. 6. Empirical eqn (2) fitted to force–velocity data obtained from a single muscle fibre: *A*, at 2·10 μm and *B*, at 2·60 μm sarcomere lengths in isotonic (1·00 *R*) Ringer solution and *C*, at 2·10 μm sarcomere length in 1·44 *R* hypertonic medium. Principle of curve fitting shown in main diagram of *A*: constants *a* and *b* in eqn (2) were determined by least-squares fitting of Hill's hyperbolic eqn (1) to data truncated at 0·78 P_0. Constants k_1 and k_2 in eqn (2) were determined by trial and error to provide best fit to experimental data at loads greater than 0·78 P_0. The same numerical values for k_1 (100 mm^2/N) and k_2 (0·82) were used in *A–C*. Insets: detail of high-force portion of the force–velocity relation shown in main diagram. Dashed line, hyperbola derived from data below 0·78 P_0. Continuous line, fit of eqn (2). Note that whereas the general shape of the force–velocity relation was markedly different in *A–C*, the same numerical values of k_1 and k_2 could be used to fit the experimental data in the high-force range in the three cases. Temperature: 1·8 °C.
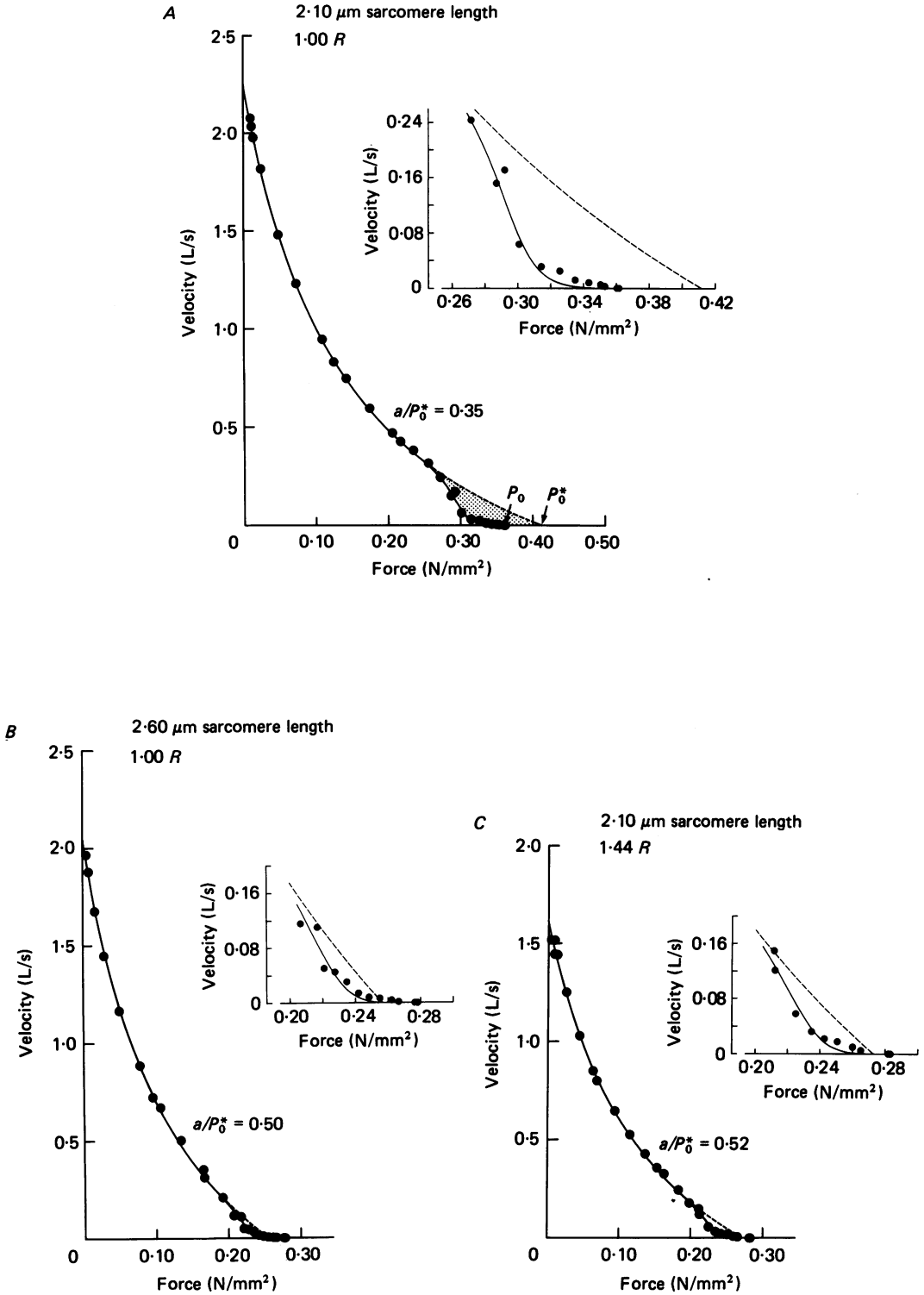
Fig. 6. For legend see opposite.

to 1·8 °C. The results demonstrate that the temperature-induced changes of the force–velocity relation were completely reversible, the second series of measurements at 1·8 °C being virtually superimposable upon the first series. V_{max} and P_0 can both be seen to increase in response to the rise in temperature, from 1·83 to 3·84 L/s and from 0·135 to 0·163 N/mm², respectively. These effects accord with the Q_{10} values for V_{max} and P_0 reported earlier (Edman, 1979). The change in temperature did not, however, affect the *shape* of the force–velocity relation to any substantial degree, neither at low–intermediate loads nor in the high-force range. The calculated value of a/P_0^* for the hyperbolic fitting at low–intermediate loads decreased by 13 % as the temperature was raised from 1·8 to 11·0 °C. The insignificant effect of temperature on the curvatures of the two sections of the force–velocity relation thus contrasts with the marked temperature dependence of V_{max}.

Curve fitting of force–velocity data

As was demonstrated in a previous study of intact muscle fibres (Edman *et al.* 1976), Hill's (1938) equation provides an excellent fit to force–velocity data truncated at 0·78 P_0. An attempt was made in the present investigation to extend the use of Hill's (1938) hyperbolic equation to also cover the high-force region of the force–velocity relation. The principle of the curve fitting at high loads is illustrated in Fig. 6A. The following function relating velocity of shortening (V) to load (P) was used:

$$V = \frac{(P_0^* - P)\,b}{P + a}\left(1 - \frac{1}{1 + e^{-k_1(P - k_2 P_0)}}\right). \tag{2}$$

The first term expresses the force–velocity curve at low and intermediate loads, i.e. at forces lower than 0·78 P_0. The constants a and b represent the asymptotes of this rectangular hyperbola and have dimensions of force and velocity, respectively, as set out in Hill's (1938) equation. P_0^* is the isometric force that is predicted from the hyperbola derived below 0·78 P_0. The second term within brackets (to be referred to as the 'correction term') reduces V in the high-force range as indicated by the dotted area in Fig. 6A. The constant k_1 in the correction term has the dimension of 1/force whereas k_2 is dimensionless. With the numerical values of k_1 and k_2 generally used (see below) the correction term assumes a value of zero (or close to zero) at low and intermediate loads. Its value changes steeply from *ca.* 0·1 to 1 as the load is increased from 0·78 P_0 to P_0. Thus, instead of the dashed portion of the force–velocity relation (predicted by plain extrapolation from the hyperbola derived at low and intermediate loads, see Fig. 6A) the equation provides a curvature of the force–velocity relation in the high-force range that agrees well with the values actually recorded.

Figure 6 illustrates force–velocity measurements from a given fibre at 2·10 μm (A) and 2·60 μm (B) sarcomere lengths in ordinary (1·00 R) Ringer solution and at 2·10 μm sarcomere length in 1·44 R hypertonic Ringer solution (C). Increasing the resting sarcomere length, or raising the tonicity of the extracellular medium, induced the characteristic changes in curvature of the force–velocity relation on either side of the break point that were described in sections 'Length dependence of force–velocity relation' and 'The force–velocity relation at varied tonicity of the extracellular medium'. The data in Fig. 6A–C have been fitted by the above
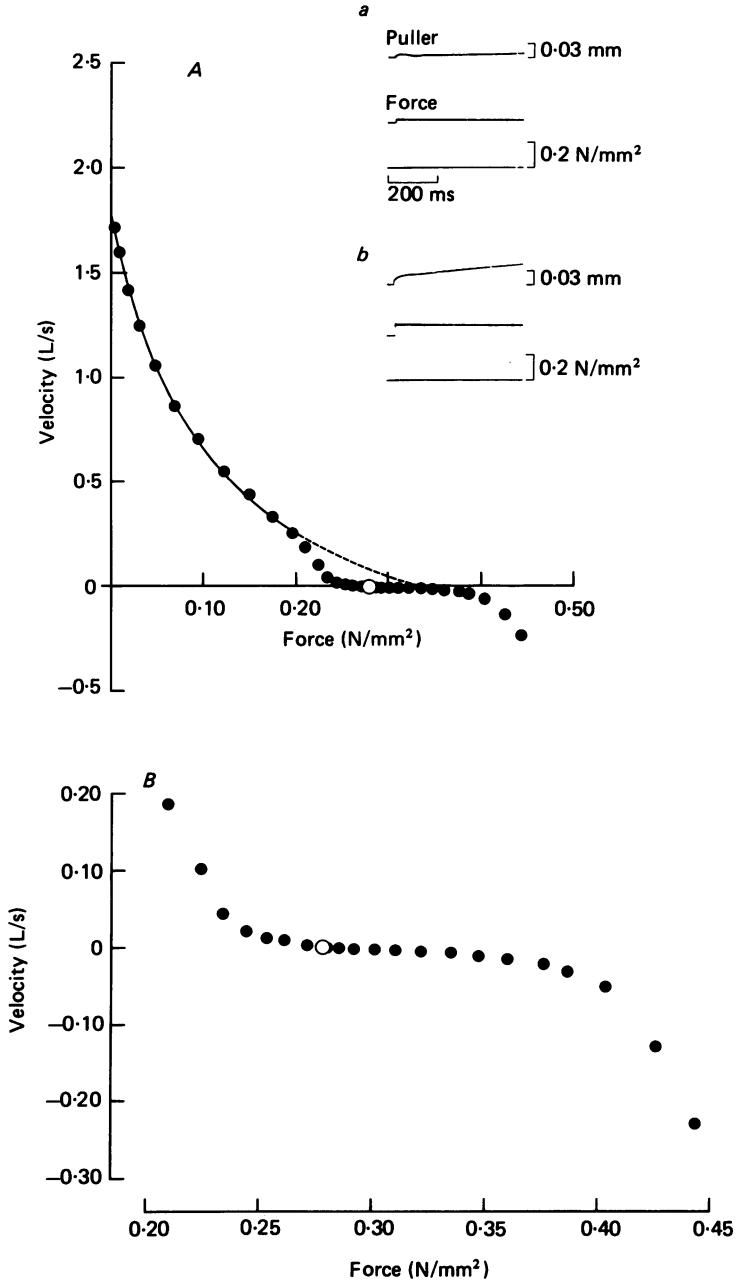
Fig. 7. *A*, force–velocity relation in a single muscle fibre including data at loads greater than the isometric force, P_0 (O). Hyperbola fitted to values truncated at $0.78\ P_0$. Insets *a* and *b*: load-clamp recordings at two different force levels greater than P_0. Traces from top: puller movement (upward, fibre elongation) and force. *B*, enlargement of the high-force portion of the force–velocity plot shown in *A*. Note smooth continuation of force–velocity relation as load passes P_0. Resting sarcomere length: $2.10\ \mu$m. Fibre length: 8.35 mm. Temperature: $1.0\ °C$.

equation using the same numerical values of k_1 and k_2 in the correction term in all three cases. It can be seen that, irrespective of the marked differences in shape of the force–velocity relationship in the three situations, the same good fit could be obtained by the equation in the high-force range in each series of measurements. Other examples of fitting eqn (2) to force–velocity data in the high-force region are presented in the insets of Fig. 3 $A–D$ and Fig. 4 A and B.

The equation was applied for curve fitting in fourteen experiments in which the force–velocity relation had been affected by changes in temperature, tonicity and sarcomere length. In these experiments the best combination of numerical values for k_1 and k_2 (tested in steps of 25 mm^2/N and 0·01, respectively) was worked out by trial and error to get as accurate curve fitting of the force–velocity relation in the high-force range as that illustrated in Figs 3, 4 and 6. The same values of k_1 and k_2 were consistently found to apply for curves recorded in any given fibre under various experimental conditions. Among the different fibres investigated the appropriate values of k_1 and k_2 were found to be within the range 100–200 mm^2/N and 0·81–0·84, respectively.

These results would seem to make clear that the two portions of the force–velocity curve are closely interrelated. Any change in curvature at low–intermediate loads is thus associated with a specific change in the high-force range so that the interrelation between the two portions is maintained constant.

Continuity of force–velocity relation as load exceeds isometric force

In a series of five experiments load-clamp recordings were performed at force levels ranging from 0·01 P_0 to 1·6–1·8 P_0, i.e. including measurements at loads exceeding the isometric force. The experiments were carried out in ordinary Ringer solution at 2·10 μm sarcomere length. Examples of load-clamp recordings at forces greater than P_0 are illustrated in Fig. 7 A (inset). Increasing the load above the isometric force caused elongation of the fibre. There was an initial rapid length change, which coincided with the tension step, and a subsequent, less rapid phase of elongation during which the tension remained at a constant level. The velocity of elongation was measured within a portion of the record (no earlier than 75 ms after the release) where the velocity was quite constant.

The results of one representative experiment are plotted in Fig. 7 A and B. The force–velocity relation, even in its extended version, can be seen to have only *one* break point, i.e. at 0·78 P_0 (see earlier). For higher tensions, including loads greater than maximum tetanic force, the force–velocity relation formed a smooth sigmoidal function with inflexion at P_0 (Fig. 7 B). There was no indication of discontinuity in the force–velocity relation around P_0 as originally inferred from measurements on whole muscle (Katz, 1939; Aubert, 1956; see Woledge *et al.* 1985 for further references). Between 0·90 and 1·20 P_0 the force–velocity curve can be seen to be nearly flat. In the five fibres investigated the velocity of shortening or elongation differed by merely 1·8 ± 0·3 % of V_{max} over this force range. Beyond 1·6 P_0 the speed of elongation increased progressively in agreement with previous studies of whole muscle (Flitney & Hirst, 1978) and single muscle fibres (Edman, Elzinga & Noble, 1981).

<center>DISCUSSION</center>

Shape of force-velocity curve

The relationship between force and velocity of shortening was explored in isolated skeletal muscle fibres of the frog using a technique that enabled measurements to be made both from the fibre as a whole and from short segments along the same intact fibre. The force-velocity curve derived in this way differs in several respects from that originally delineated in studies of whole muscle (Fenn & Marsh, 1935; Hill, 1938). The new results confirm that the force-velocity curve has a break point near 78 % of the isometric force (cf. Edman *et al.* 1976) and they furthermore demonstrate that the force-velocity relation contains *two* distinct regions, each one with an upward concavity, located on either side of the break point. The two sections of the curve can individually be fitted quite well by a rectangular hyperbola or by an exponential function. It should be noted, however, that neither of these functions provides a completely faithful description of the force-velocity relation as the measured values regularly exhibit small systematic deviations from the theoretical curves (Figs 2-6, see also Fig. 8 in Edman *et al.* 1976).

It appears unlikely that the biphasic shape of the force-velocity curve is due to non-uniform contractile behaviour along the fibre. In order to explain the sharp decline in shortening velocity at high loads on this basis, it would be necessary to assume that part of the fibre would fail to shorten and start to elongate as soon as the load exceeds a given level, i.e. 75-80 % of P_0. Local differences in contractile strength do exist along a muscle fibre as demonstrated by length clamping short consecutive segments of the intact fibre (Edman & Reggiani, 1984; Edman, Reggiani & te Kronnie, 1985). These differences, however, are quite small (see Fig. 3*A* in Edman *et al.* 1985) and would not be expected to cause any marked redistribution of length along the fibre during load-clamp recording in the high-force range. This conclusion is substantiated by the present results which show that the force-velocity curve has the same features irrespective of whether the measurements are made from the fibre as a whole or from a short segment of the same fibre (Fig. 2). This finding suggests strongly that the double curvature of the force-velocity relation, with a break point near $0.78\,P_0$, does represent contractile behaviour at the sarcomere level.

Nature of biphasic shape of force-velocity curve

A modified version of Hill's (1938) hyperbolic equation (see page 314) was used to fit the experimental data. The equation operates as a rectangular hyperbola at low and intermediate loads but includes an additional function that accounts for the departure of the force-velocity data from this hyperbola in the high-force range. The equation provides a useful method to evaluate the interrelation between the two portions of the force-velocity curve. The results show that the two curvatures are closely related to one another. The interrelation between the two portions was found to be nearly the same from fibre to fibre and to remain constant in any given fibre under different experimental conditions that altered the general shape of the force-velocity curve. A change in curvature of the force-velocity relation at

low–intermediate loads was thus found to be associated with a given change in shape of the curve in the high-force range. These findings provide evidence that the kinetics of the contractile process does change in a specific way as the load on the muscle exceeds a critical level.

According to the most widely accepted view (Huxley & Niedergerke, 1954; Huxley & Hanson, 1954; Huxley, 1957; Huxley, 1969) active force production in muscle is based on cyclic interaction of myosin cross-bridges with the thin filaments. In this process the myosin bridges are thought to act as independent force generators, i.e. the performance of any one bridge is assumed to be uninfluenced by the activity of other bridges. The mechanical behaviour of the contractile system under lightly loaded conditions is in accord with this view. Thus, as demonstrated in intact single muscle fibres (Edman, 1979), the speed of shortening at zero load is unaffected by changes in sarcomere length and state of activation of the contractile system, interventions that are both likely to alter the number of cross-bridges available for interaction with the thin filament. The biphasic shape of the force–velocity curve could mean that the independent character of the cross-bridges is lost in the high-force range as the density of attached cross-bridges exceeds a certain level. The possibility exists that a high density of attached bridges imposes some restriction upon the unattached bridges in their search for a suitable binding site on the actin filament. That is, the association rate constant of the myosin bridges may be progressively reduced as the load is increased beyond the break point of the force–velocity curve. By including this assumption in A. F. Huxley's (1957) cross-bridge model it is indeed possible to simulate the observed increase in curvature of the force–velocity relation in the high-force range (K. A. P. Edman & A. Månsson, unpublished data). In a cross-bridge model including two or more attached states (Huxley & Simmons, 1971; Eisenberg & Hill, 1978) the increased steepness of the force–velocity curve at high loads may be accounted for by a larger fraction of bridges going into a state of low force production as the density of attached bridges becomes sufficiently high.

Another, more speculative possibility to explain the altered shape of the force–velocity relation at high loads would be that, in addition to the 'normal' population of cross-bridges, there exists a fraction of bridges that operate against the sliding movement. If these 'abnormal' bridges have a low attachment rate, they would come into action only at high loads when the sliding motion is sufficiently low. However, a mechanism of this kind appears unlikely in view of the fact that both actin and myosin filaments have a polarity that favours force production in one direction only, i.e. the force exerted on the thin filament is towards the centre of the sarcomere (Huxley, 1969).

Influence of sarcomere length and fibre width on force–velocity characteristics

The present results confirm the previous observation (Edman, 1979) that V_{max}, the maximum velocity of shortening, remains constant over a wide range (1·7–2·7 μm) of sarcomere lengths. This is an interesting finding as it would seem to imply that V_{max} is insensitive not only to changes in filament overlap but also to variations in myofilament lattice width. As the volume of an intact muscle fibre is maintained constant during a length change (for references, see earlier), the amount of filament

overlap and the side-to-side distance between the filaments will both vary with the sarcomere spacing, the former as a linear function, the latter as an inverse square root function of the sarcomere length. The fact that V_{max} is constant over the entire range from 1·7 to 2·7 μm sarcomere length (corresponding to a 21 % decrease in myofilament lattice width) thus leads to the conclusion that V_{max} is not critically dependent on the lateral spacing between the A and I filaments in the intact muscle fibre. The alternative interpretation would be that changes in filament overlap and myofilament lattice width both affect V_{max} but in such a way that the two effects just cancel out one another at each sarcomere length. A mechanism of this kind appears highly unlikely considering the fact that the two parameters vary as quite different functions of sarcomere length (see above). Further evidence against such a dual influence of sarcomere length on V_{max} is provided by the finding that maximum speed of shortening is independent of sarcomere length also in skinned muscle fibres (Julian, 1971; Thames, Teichholz & Podolsky, 1974). In the skinned preparation, contrary to the situation in the intact fibre, the myofilament lattice width remains virtually constant as the sarcomere length is changed (Matsubara & Elliott, 1972; Matsubara, Goldman & Simmons, 1984).

The problem whether V_{max} is dependent on the width of the myofilament lattice has recently been taken up in experiments on skinned muscle fibres (Goldman, 1987; Metzger & Moss, 1987; Tsuchiya, 1988). In these studies the degree of hydration, and therefore the width of the myofilament lattice, was reduced by immersing the fibres in solutions containing macromolecules (polyvinylpyrrolidine, sucrose) that were large enough to be excluded from the myofibrillar space. The results of these studies show that osmotic compression of the skinned fibre causes a steady reduction of V_{max}. At the present time it is not possible to decide whether the observed change of V_{max} in the skinned fibre is attributable to the change in fibre diameter, or to the decrease in the water contents *per se* in the myofibrillar space. The latter possibility needs to be considered in view of the fact that no effect on V_{max} of altered width is detectable in the intact muscle fibre under conditions where the volume of the fibre is kept constant (see above). It should be noted in this connection that osmotic compression of the intact fibre (induced by increased tonicity of the extracellular medium) leads to a decrease of V_{max} similar to that observed in the skinned preparation (Fig. 4 and Edman & Hwang, 1977).

The *shape* of the force–velocity relation, as distinguished from V_{max}, is clearly dependent on sarcomere length in the intact muscle fibre. An increase in sarcomere spacing from 2·10 to 2·60 μm was thus found to be associated with a decrease in curvature of the force–velocity relation, both at low–intermediate loads and in the high-force range. This change in shape of the force–velocity curve is most likely attributable to the decrease in width of the myofilament lattice that occurs as the sarcomere length is increased. This is supported by the observation that the same change in shape of the force–velocity curve is obtained as the fibre diameter is reduced to an equivalent degree by osmotic compression of the fibre in a hypertonic medium (Table 1). A decrease in curvature of the force–velocity relation is likewise produced by osmotic compression of the skinned fibre preparation (Goldman, 1987).

The present results thus support the view that the width of the myofilament lattice

is not of significance for the maximum speed of shortening of the contractile system. This would mean, in terms of A. F. Huxley's (1957) cross-bridge model, that g_2, the rate constant for bridge dissociation at negative strain, is independent of the lateral distance between the myofilaments within the range studied. The width of the myofilament lattice does, on the other hand, seem to affect the *shape* of the force–velocity curve. The observed change in shape of the force–velocity curve (increase of a/P_0 with decreasing fibre diameter) would be explainable in Huxley's model by assuming that the sum of f_1 and g_1, representing the rate constants for attachment and detachment of cross-bridges at positive strain, respectively, is increased as the side-to-side distance between the A and I filaments is reduced.

REFERENCES

ARMSTRONG, C. F., HUXLEY, A. F. & JULIAN, F. J. (1966). Oscillatory responses in frog skeletal muscle fibres. *Journal of Physiology* **186**, 26–27P.

AUBERT, X. (1956). *Le Couplage Énergétique de la Contraction Musculaire.* Brussels: Arscia.

BLINKS, J. R. (1965). Influence of osmotic strength on cross-section and volume of isolated single muscle fibres. *Journal of Physiology* **177**, 42–57.

CIVAN, M. M. & PODOLSKY, R. J. (1966). Contraction kinetics of striated muscle fibres following a quick change in load. *Journal of Physiology* **184**, 511–534.

CLEWORTH, D. R. & EDMAN, K. A. P. (1972). Changes in sarcomere length during isometric tension development in frog skeletal muscle. *Journal of Physiology* **227**, 1–17.

EDMAN, K. A. P. (1979). The velocity of unloaded shortening and its relation to sarcomere length and isometric force in vertebrate muscle fibres. *Journal of Physiology* **291**, 143–159.

EDMAN, K. A. P. (1986). Further characterization of the force–velocity relation in frog skeletal muscle. *Journal of Physiology* **377**, 92P.

EDMAN, K. A. P. (1988). Double-hyperbolic nature of the force–velocity relation in frog skeletal muscle. In *Molecular Mechanism of Muscle Contraction*, ed. SUGI, H. & POLLACK, G. H. New York: Plenum Press (in the Press).

EDMAN, K. A. P., ELZINGA, G. & NOBLE, M. I. M. (1981). Critical sarcomere extension required to recruit a decaying component of extra force during stretch in tetanic contraction of frog skeletal muscle fibres. *Journal of General Physiology* **78**, 365–382.

EDMAN, K. A. P. & HWANG, J. C. (1977). The force–velocity relationship in vertebrate muscle fibres at varied tonicity of the extracellular medium. *Journal of Physiology* **269**, 255–272.

EDMAN, K. A. P., MULIERI, L. A. & SCUBON-MULIERI, B. (1976). Non-hyperbolic force–velocity relationship in single muscle fibres. *Acta physiologica scandinavica* **98**, 143–156.

EDMAN, K. A. P. & REGGIANI, C. (1984). Redistribution of sarcomere length during isometric contraction of frog muscle fibres and its relation to tension creep. *Journal of Physiology* **351**, 169–198.

EDMAN, K. A. P., REGGIANI, C. & TE KRONNIE, G. (1985). Differences in maximum velocity of shortening along single muscle fibres of the frog. *Journal of Physiology* **365**, 147–163.

EISENBERG, E. & HILL, T. L. (1978). A cross-bridge model of muscle contraction. *Progress in Biophysics and Molecular Biology* **33**, 55–82.

ELLIOTT, G. F., LOWY, J. & MILLMAN, B. M. (1967). Low-angle X-ray diffraction studies of living striated muscle during contraction. *Journal of Molecular Biology* **25**, 31–45.

ELLIOTT, G. F., LOWY, J. & WORTHINGTON, C. R. (1963). An X-ray and light-diffraction study of the filament lattice of striated muscle in the living state and in rigor. *Journal of Molecular Biology* **6**, 295–305.

FENN, W. O. & MARSH, B. S. (1935). Muscular force at different speeds of shortening. *Journal of Physiology* **85**, 277–297.

FLITNEY, F. W. & HIRST, D. G. (1978). Cross-bridge detachment and sarcomere 'give' during stretch of active frog's muscle. *Journal of Physiology* **276**, 449–465.

GOLDMAN, Y. E. (1987). Measurement of sarcomere shortening in skinned fibers from frog muscle by white light diffraction. *Biophysical Journal* **52**, 57–68.

HILL, A. V. (1938). The heat of shortening and the dynamic constants of muscle. *Proceedings of the Royal Society* B **126**, 136–195.

HOWARTH, J. V. (1958). The behaviour of frog muscle in hypertonic solutions. *Journal of Physiology* **144**, 167–175.

HUXLEY, A. F. (1957). Muscle structure and theories of contraction. *Progress in Biophysics and Biophysical Chemistry* **7**, 255–318.

HUXLEY, A. F. & NIEDERGERKE, R. (1954). Interference microscopy of living muscle fibres. *Nature* **173**, 971–973.

HUXLEY, A. F. & SIMMONS, R. M. (1971). Proposed mechanism of force generation in striated muscle. *Nature* **233**, 533–538.

HUXLEY, H. E. (1953). X-ray analysis and the problem of muscle. *Proceedings of the Royal Society* B **141**, 59–62.

HUXLEY, H. E. (1969). The mechamism of muscular contraction. *Science* **164**, 1356–1366.

HUXLEY, H. E. & HANSON, J. (1954). Changes in the cross-striations of muscle during contraction and stretch and their structural interpretation. *Nature* **173**, 973–976.

JEWELL, B. R. & WILKIE, D. R. (1958). An analysis of the mechanical components in frog's striated muscle. *Journal of Physiology* **143**, 515–540.

JULIAN, F. J. (1971). The effect of calcium on the force–velocity relation of briefly glycerinated frog muscle fibres. *Journal of Physiology* **218**, 117–145.

KATZ, B. (1939). The relation between force and speed in muscular contraction. *Journal of Physiology* **96**, 45–64.

MATSUBARA, I. & ELLIOTT, G. F. (1972). X-ray diffraction studies on skinned single fibres of frog skeletal muscle. *Journal of Molecular Biology* **72**, 657–669.

MATSUBARA, I., GOLDMAN, Y. E. & SIMMONS, R. M. (1984). Changes in the lateral filament spacing of skinned muscle fibres when cross-bridges attach. *Journal of Molecular Biology* **173**, 15–33.

METZGER, J. M. & MOSS, R. L. (1987). Shortening velocity in skinned single muscle fibers, influence of filament lattice spacing. *Biophysical Journal* **52**, 127–131.

RITCHIE, J. M. & WILKIE, D. R. (1958). The dynamics of muscular contraction. *Journal of Physiology* **143**, 104–113.

SUGI, H. & TSUCHIYA, T. (1981). Isotonic velocity transients in frog muscle fibres following quick changes in load. *Journal of Physiology* **319**, 219–238.

THAMES, M. D., TEICHHOLZ, L. E. & PODOLSKY, R. J. (1974). Ionic strength and the contraction kinetics of skinned muscle fibers. *Journal of General Physiology* **63**, 509–530.

TSUCHIYA, T. (1988). Passive interaction between sliding filaments in the osmotically compressed skinned muscle fibers of the frog. *Biophysical Journal* **53**, 415–423.

WOLEDGE, R. C., CURTIN, N. A. & HOMSHER, E. (1985). *Energetic Aspects of Muscle Contraction.* London: Academic Press.